

Figure 1. Static structures for  $\text{Sn}_9^{4-}$ .

of  $\text{Sn}_9^{4-}$  and has predicted nonrigidity.<sup>1</sup> Our experiments confirm this expectation.

We also have found from  $^{119}\text{Sn}$  NMR that the extraction of Na-Sn-Pb and Na-Sn-Sb alloy with en gives solutions containing new clusters in addition to  $\text{Sn}_9^{4-}$ . The en solutions obtained from the Na-Sn-Pb alloy contain at least six new clusters observable by  $^{119}\text{Sn}$  NMR. Each cluster gives a distinct multiplet to the high-field side of  $\text{Sn}_9^{4-}$  with the displacement of successive multiplets gradually increasing from 42 to 60 ppm. Although the signal-to-noise ratio for these signals is poorer at higher field, our analysis of the multiplet patterns<sup>5,8</sup> indicates that they arise from  $(\text{PbSn}_8)^{4-}$ ,  $(\text{Pb}_2\text{Sn}_7)^{4-}$ ,  $(\text{Pb}_3\text{Sn}_6)^{4-}$ ,  $(\text{Pb}_4\text{Sn}_5)^{4-}$ ,  $(\text{Pb}_5\text{Sn}_4)^{4-}$ , and  $(\text{Pb}_6\text{Sn}_3)^{4-}$  clusters, respectively. Each multiplet shows  $^{119}\text{Sn}$ - $^{117}\text{Sn}$  coupling of  $\sim 260$  Hz and  $^{119}\text{Sn}$ - $^{207}\text{Pb}$  coupling of  $\sim 560$  Hz. The  $^{207}\text{Pb}$  NMR<sup>4</sup> at 16.591 MHz shows the clusters  $(\text{Pb}_3\text{Sn}_6)^{4-}$ ,  $(\text{Pb}_4\text{Sn}_5)^{4-}$ ,  $(\text{Pb}_5\text{Sn}_4)^{4-}$ ,  $(\text{Pb}_6\text{Sn}_3)^{4-}$ ,  $(\text{Pb}_7\text{Sn}_2)^{4-}$ ,  $(\text{Pb}_8\text{Sn})^{4-}$ , and  $(\text{Pb}_9)^{4-}$  with the latter at 1190.9 ppm upfield from 1 M  $\text{Pb}(\text{NO}_3)_2$  and successive displacements to lower field of  $\sim 185$  ppm/Sn atom.

The Na-Sn-Sb alloy yields a new cluster 108.1 ppm downfield from  $\text{Sn}_9^{4-}$  with  $J_{^{119}\text{Sn}-^{117}\text{Sn}} = 84$  Hz and relative intensities indicative of nine tin atoms in the new cluster. No evidence of  $^{119}\text{Sn}$ - $^{121}\text{Sb}$  or  $^{119}\text{Sn}$ - $^{123}\text{Sb}$  coupling has been observed. Therefore, NMR cannot establish the number of Sb atoms in the new cluster, and antimony may be exchanging rapidly on the NMR time scale. Isolation is currently being attempted; however, it is interesting to speculate regarding the nature of the cluster. For instance, the PERC<sup>9</sup> approach would suggest either  $\text{SbSn}_9^{3-}$  or  $\text{SbSn}_9^-$  if a single Sb atom per cluster is present. The latter is expected to have a bicapped square antiprism structure, the former a more open structure.

**Acknowledgment.** The support of this work with a Rackham Grant (University of Michigan) is sincerely appreciated. We also wish to thank the Matilda R. Wilson Fund for a generous grant for the purchase of an FT NMR spectrometer (Oakland University).

## References and Notes

- See (a) J. D. Corbett and P. A. Edwards, *J. Am. Chem. Soc.*, **99**, 3313 (1977); (b) C. H. E. Belin, J. D. Corbett, and A. Cisar, *ibid.*, **99**, 7163 (1977).
- 4,7,13,16,21,24-Hexaoxa-1,10-diazobicyclo[8.8.8]hexacosane,  $\text{N}(\text{C}_2\text{H}_4\text{-OC}_2\text{H}_4\text{OC}_2\text{H}_4)_3\text{N}$ : J. M. Lehn and J. P. Sauvage, *J. Am. Chem. Soc.*, **97**, 6700 (1975).
- D. Kummer and L. Diehl, *Angew. Chem., Int. Ed. Engl.*, **9**, 895 (1970); L. Diehl, K. Khodadadeh, D. Kummer, and J. Stahle, *Z. Naturforsch. B*, **31**, 522 (1976); *Chem. Ber.*, **109**, 3404 (1976).
- For leading references regarding  $^{119}\text{Sn}$  and  $^{207}\text{Pb}$  chemical shifts, relaxation times, and FT methods, etc., see R. R. Sharp and J. Tolani, *J. Chem. Phys.*, **65**, 522 (1976); G. E. Maciel in "NMR of Nuclei other than Protons", T. Axenrod and G. A. Webb, Ed., Wiley, New York, N.Y., 1974; C. R. Lassigne and E. J. Wells, *Can. J. Chem.*, **55**, 927 (1977).
- These calculations are based on abundances of 8.58 and 7.61% for  $^{119}\text{Sn}$  and  $^{117}\text{Sn}$ , respectively. Only the five central lines are listed because the outer lines are too low in intensity for detection. Theoretically, 15-, 17-, and 19-line patterns are predicted for 8-, 9-, and 10-atom clusters, respectively. The calculated relative intensities of the multiplet pattern vary significantly with the size of the cluster; e.g., the five central lines for a 8, 9, and 10-atom cluster are calculated to be 0.034:0.276:1.000:0.276:0.034, and 0.044:0.311:1.000:0.311:0.044, and 0.056:0.345:1.000:0.345:0.056, respectively.

- We discount the possibility that all cluster environments are coincidentally at the same chemical shift.
- T. N. Mitchell, *J. Organomet. Chem.*, **70**, C1 (1974).
- The relative intensity pattern of the  $^{119}\text{Sn}$  and  $^{207}\text{Pb}$  NMR can establish cluster stoichiometry but not anionic charge.  $^{23}\text{Na}$  NMR gives a single resonance and thus doesn't solve the problem. The anionic charge is inferred from the observed systematic variation in chemical shift as Pb is substituted for Sn.
- R. W. Rudolph, *Acc. Chem. Res.*, **9**, 446 (1976).

R. W. Rudolph,\* W. L. Wilson, F. Parker

Department of Chemistry, University of Michigan  
Ann Arbor, Michigan 48109

R. Craig Taylor, D. C. Young

Department of Chemistry, Oakland University  
Rochester, Michigan 48063

Received March 30, 1978

## The Molybdenum-Iron-Sulfur Cluster Complex $[\text{Mo}_2\text{Fe}_6\text{S}_9(\text{SC}_2\text{H}_5)_8]^{3-}$ . A Synthetic Approach to the Molybdenum Site in Nitrogenase

Sir:

EXAFS (extended x-ray absorption fine structure) spectroscopy of FeMo proteins of nitrogenase<sup>1</sup> and of the FeMo cofactor<sup>2</sup> ( $\text{FeMo-co}$ ) isolated therefrom<sup>3</sup> has demonstrated that the molybdenum coordination sites in these species are distinctly similar, and has implicated molybdenum in a Mo-Fe-S cluster unit as yet undefined in detail. Noting the spontaneous self-assembly of the ferredoxin analogue clusters  $[\text{Fe}_4\text{S}_4(\text{SR})_4]^{2-}$  from simple reagents,<sup>4</sup> a similar approach to the synthesis of Mo-Fe-S clusters is under investigation by us. Anaerobic reaction of 1 equiv of  $(\text{Et}_4\text{N})_2\text{MoS}_4$ , 3 equiv of  $\text{FeCl}_3$ , and 9 equiv each of ethanethiol and NaOMe in methanol afforded, after unexceptional workup and recrystallization from acetonitrile-THF, black crystals whose composition is consistent with the formulation  $(\text{Et}_4\text{N})_3[\text{Mo}_2\text{Fe}_6\text{S}_9(\text{SEt})_8]$ :<sup>5</sup>  $\lambda_{\text{max}}$  274 nm ( $\epsilon_M$  58 100), 395 (38 000) in DMF.

The compound crystallizes as hexagonal rods in space group  $P6_3/m$  with  $a = b = 17.230$  (6),  $c = 15.999$  (4) Å;  $V = 4113$  Å<sup>3</sup>; and  $Z = 2$ .<sup>6</sup> Data collected on a Syntex P2<sub>1</sub> diffractometer using graphite monochromatized Mo K $\alpha$  radiation yielded 800 unique reflections with  $F_o^2 > 3\sigma(F_o)^2$  out to  $2\theta$  of 50°. The structure (Figure 1) was solved by MULTAN and refined by standard procedures; at the current refinement stage  $R = 5.6\%$  and  $R_w = 8.6\%$ . Two molybdenum atoms, each in a  $\text{MoFe}_3\text{S}_4$  cubane-type cluster, are bridged by three sulfur atoms across the mirror plane at  $z = 1/4$  in  $P6_3/m$ . All atomic positions except for those of the bridging atoms were readily determined. Fourier and difference Fourier maps of the bridging region revealed electron density elongated in the mirror plane and attributable to sulfur atoms of SEt groups with partial occupancy. This density was satisfactorily refined in terms of the  $\text{Mo}(\mu\text{-S})(\mu\text{-SEt})_2\text{Mo}$  unit whose bridging groups are disordered by the crystallographic threefold axis.<sup>7</sup>

The presence of two (but not one or three)  $\mu\text{-SEt}$  groups in the 3 anion requires a paramagnetic ground state and is further supported by these observations; (i)  $\mu = 4.83 \mu_B$  at 4.2 K and  $H_0 = 3.890$  kOe; (ii) magnetic hyperfine  $^{57}\text{Fe}$  Mössbauer spectrum at 4.2 K and  $H_0 = 60\text{--}80$  kOe (consisting of two superimposed spectra with opposite hyperfine interactions of ca.  $-210$  and  $+150$  kOe); (iii) strong EPR spectrum with apparent  $g$  values near  $\sim 10$ , 4.0, 1.9, and 1.2 (4.2 K, DMF); (iv) isotropically shifted  $^1\text{H}$  NMR spectrum with signals at 54.2 ppm downfield and 3.1 ppm upfield of  $\text{Me}_4\text{Si}$  in a  $\sim 3:1$  intensity ratio ( $\text{CD}_3\text{CN}$ ,  $\sim 25^\circ\text{C}$ ) (these signals are tentatively assigned to the Fe-SCH<sub>2</sub> and Mo-SCH<sub>2</sub> units, respectively). The Mössbauer spectrum in zero magnetic field consists of a

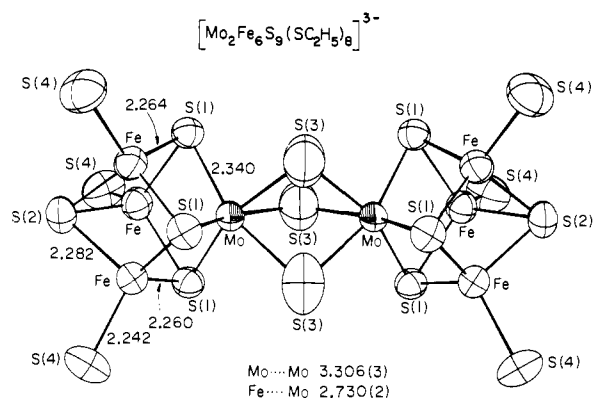


**Figure 1.** Structure of  $[\text{Mo}_2\text{Fe}_6\text{S}_9(\text{SEt})_8]^{3-}$  as its  $\text{Et}_4\text{N}^+$  salt; the two disordered ethyl groups in the  $\text{MoS}(\text{SEt})_2\text{Mo}$  bridge unit and those of the six terminal thiolate ligands are given elsewhere.<sup>1,9</sup> A more direct comparison of the contribution to the EXAFS of the short Mo-S and the Mo-Fe interactions within one cluster is shown on the right. The close agreement between the sum of the Mo-S plus Mo-Fe components (and, likewise, the very close agreement between the parameters<sup>10</sup> determined from the fits) established that the FeMo protein possesses Mo to S and Fe interactions that dictate the presence of a structural fragment similar to the  $\text{MoFe}_3\text{S}_4$  cube that constitutes one half of the complex  $[\text{Mo}_2\text{Fe}_6\text{S}_9(\text{SEt})_8]^{3-}$ .

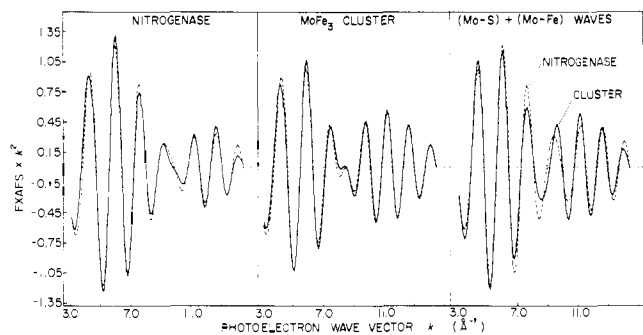


**Figure 2.** Curve-fitting analysis of Mo EXAFS for the FeMo protein of *Clostridium pasteurianum* (left) and  $[\text{Mo}_2\text{Fe}_6\text{S}_9(\text{SEt})_8]^{3-}$  (center). In each case the data (—) are fit (---) using three waves: Mo-S, Mo-Fe, and Mo-S'. Details of the fitting method are given elsewhere.<sup>1,9</sup> A more direct comparison of the contribution to the EXAFS of the short Mo-S and the Mo-Fe interactions within one cluster is shown on the right. The close agreement between the sum of the Mo-S plus Mo-Fe components (and, likewise, the very close agreement between the parameters<sup>10</sup> determined from the fits) established that the FeMo protein possesses Mo to S and Fe interactions that dictate the presence of a structural fragment similar to the  $\text{MoFe}_3\text{S}_4$  cube that constitutes one half of the complex  $[\text{Mo}_2\text{Fe}_6\text{S}_9(\text{SEt})_8]^{3-}$ .

single slightly asymmetric quadrupole doublet with somewhat broadened lines; at 77 K,  $\delta$  is  $0.27 \pm 0.02$ ,  $\Delta E_Q = 0.95 \pm 0.03$ , and  $\Gamma_{1/2} = 0.31$  mm/s. Isomer shifts of other Fe-S complexes<sup>8</sup> vary nearly linearly with formal oxidation state ( $\delta_{\text{Fe(II)}} - \delta_{\text{Fe(III)}} \approx 0.47$  mm/s, source and absorber at 77 K). Interpolation of the observed  $\delta$  value gives  $\text{Fe}^{+2.67}$ , or a formal  $2\text{Fe(III)} + \text{Fe(II)}$  configuration. From this result it follows that the molybdenums in  $[\text{Mo}_2\text{Fe}_6\text{S}_9(\text{SEt})_8]^{3-}$  are also formally mixed valence (very likely  $\text{Mo(III)} + \text{Mo(IV)}$ ); however, the molybdenum sites are symmetry related in the crystal structure.

Molybdenum K-edge x-ray absorption data on  $(\text{Et}_4\text{N})_3[\text{Mo}_2\text{Fe}_6\text{S}_9(\text{SEt})_8]$  were collected using previous methods<sup>1,9</sup> and curve-fitting analysis of the EXAFS was performed in a manner identical with that described previously.<sup>9</sup> Initial fitting to the EXAFS data assuming two coordination shells (Mo-S, Mo-Fe) was very unsatisfactory. Addition of a third shell (Mo-S') reduced the fit residual by threefold and gave the excellent fit in Figure 2, center. Calculated from the EXAFS analysis were 3.7 S and 2.2 S' atoms at 2.35 and 2.55 Å, respectively, from Mo and a Mo-Fe distance of 2.76 Å. These results further verify the  $\text{Mo}(\mu\text{-S})(\mu\text{-SEt})_2\text{Mo}$  bridge and provide individual Mo-S distances unavailable from crystallography owing to disorder.

One proposed structure for the molybdenum site in FeMo proteins, derived from curve-fitting analysis of the Mo EXAFS

analogous to that employed here, was a cubane-type  $\text{MoFe}_3\text{S}_4$  cluster.<sup>1</sup> The protein and  $[\text{Mo}_2\text{Fe}_6\text{S}_9(\text{SEt})_8]^{3-}$  EXAFS data and the fits used to obtain Mo-S, Mo-S', and Mo-Fe distances are shown in Figure 2. Striking similarities can be seen in Figure 2, right, which compares the sum of the Mo-Fe and the shorter Mo-S waves from each of the two fits. Differences near  $k \sim 8 \text{ \AA}^{-1}$  result from slightly different Mo-Fe distances and Mo-S amplitudes. Actual distances and numbers of atoms in each shell derived from the fits are extremely similar for the proteins<sup>10</sup> and  $[\text{Mo}_2\text{Fe}_6\text{S}_9(\text{SEt})_8]^{3-}$ .

These results show that  $[\text{Mo}_2\text{Fe}_6\text{S}_9(\text{SEt})_8]^{3-}$  possesses a molybdenum structural fragment in common with FeMo proteins<sup>1</sup> and FeMo-co,<sup>2</sup> both of which, therefore, contain Mo-Fe and Mo-S interactions at distances similar to those in the synthetic species. Because the EXAFS of  $[\text{Mo}_2\text{Fe}_6\text{S}_9(\text{SEt})_8]^{3-}$  does not reflect the presence of the more distant S(2) atom (Figure 1), it is not possible to assert that the complete  $\text{MoFe}_3\text{S}_4$  cluster is present in the proteins or cofactors. For this reason and because of differences in Fe:S:Mo atom ratios and in certain spectroscopic properties between FeMo proteins,<sup>11</sup> FeMo-co,<sup>3,12</sup> and  $[\text{Mo}_2\text{Fe}_6\text{S}_9(\text{SEt})_8]^{3-}$ , the latter in its entirety cannot be designated as a true analogue of molybdenum sites in nitrogenase. It is, however, the closest synthetic approach to these sites yet available.

**Acknowledgments.** We thank Drs. S. P. Cramer and E. J. Laskowski for experimental assistance. This research was supported by NSF Grants PCM 17105 and CHE 77-04397 at Stanford University and by the National Science Foundation at M.I.T.

## References and Notes

- S. P. Cramer, K. O. Hodgson, W. O. Gillum, and L. E. Mortenson, *J. Am. Chem. Soc.*, **100**, 3398 (1978).
- S. P. Cramer, W. O. Gillum, K. O. Hodgson, L. E. Mortenson, E. I. Stiefel, J. R. Chisnell, W. J. Brill, and V. K. Shah, *J. Am. Chem. Soc.*, in press.
- V. K. Shah and W. J. Brill, *Proc. Natl. Acad. Sci. U.S.A.*, **74**, 3249 (1977).
- B. A. Averill, T. Herskovitz, R. H. Holm, and J. A. Ibers, *J. Am. Chem. Soc.*, **95**, 3523 (1973).
- Anal. Calcd for  $\text{C}_{40}\text{H}_{100}\text{Fe}_6\text{Mo}_2\text{N}_3\text{S}_{17}$ : C, 28.34; H, 5.95; Fe, 19.77; Mo, 11.32; N, 2.48; S, 32.15. Found: C, 28.42; H, 5.95; Fe, 19.18; Mo, 10.93; N, 2.48; S, 32.32.
- The systematic absences  $000l, l = 2n$ , are consistent with space groups  $P6_3$ ,  $P6_3/m$ , and  $P6_322$ . Statistical analysis of the intensity data suggested the centric group, and structural refinement in  $P6_3/m$  confirmed this as the correct choice.
- The limited range of data prevented resolution of the two different distances from Mo to the disordered S atoms in the mirror plane. The disorder was modeled by allowing one S atom to refine anisotropically; this atom assumed a root mean square amplitude of  $\sim 0.55 \text{ \AA}^2$  in the mirror plane with the density clearly extending toward the ethyl group. Setting the occupancy of the ethyl C atoms as if there were two groups distributed over the three positions resulted in refinement of the isotropic methylene  $\beta$  carbons to a value of  $\sim 5.0 \text{ \AA}^2$ . The same procedure assuming one ethyl group resulted in an abnormally low  $\beta$  value of  $\sim 1.0 \text{ \AA}^2$ .
- $[\text{Fe}(\text{SCH}_2)_2\text{C}_6\text{H}_4]_2^{1-2-}$ : R. W. Lane, J. A. Ibers, R. B. Frankel, G. C. Papaefthymiou, and R. H. Holm, *J. Am. Chem. Soc.*, **99**, 84 (1977).  $[\text{Fe}_2\text{S}_2(\text{SCH}_2)_2\text{C}_6\text{H}_4]_2^{2-}$ : W. O. Gillum, R. B. Frankel, S. Foner, and R. H. Holm, *Inorg. Chem.*, **15**, 1095 (1976).  $[\text{Fe}_4\text{S}_4(\text{SR})_4]^{2-}$ : R. B. Frankel, B. A. Averill, and R. H. Holm, *J. Phys. (Paris)*, **35**, C6-107 (1974).  $[\text{Fe}_4\text{S}_4(\text{SR})_4]^{3-}$ : E. J. Laskowski, R. B. Frankel, J. A. Ibers, W. O. Gillum, G. C. Papaefthymiou, J. Renaud, and R. H. Holm, *J. Am. Chem. Soc.*, in press.
- S. P. Cramer, K. O. Hodgson, E. I. Stiefel, and W. E. Newton, *J. Am. Chem. Soc.*, **100**, 2748 (1978).
- The curve-fitting analysis utilized two parameters for each shell of atoms surrounding the absorber. The overall amplitude multiplier,  $C_0$ , contained the number of atoms in the shell and the distance was obtained from the linear part ( $a_1$ ) of the phase. For both  $[\text{Mo}_2\text{Fe}_6\text{S}_9(\text{SEt})_8]^{3-}$  and nitrogenase, the EXAFS is adequately described by three ligand shells surrounding the Mo. The first two shells (Mo-S and Mo-Fe) account for about 85% of the EXAFS. The numerical values derived from the fits for these two shells for  $[\text{Mo}_2\text{Fe}_6\text{S}_9(\text{SEt})_8]^{3-}$  and for nitrogenase (in brackets) are as follows: Mo-S, 3.65 [3.79] sulfur atoms at 2.35 [2.35] Å; Mo-Fe, 3.00 [3.01] iron atoms at 2.76 [2.72] Å. As discussed elsewhere<sup>1,9,13</sup> distances determined by this method are accurate to ca.  $\pm 0.03 \text{ \AA}$  and coordination numbers to ca. 20%.
- E. Münck, H. Rhodes, W. H. Orme-Johnson, L. C. Davis, W. J. Brill, and V. K. Shah, *Biochim. Biophys. Acta*, **400**, 32 (1975); W. H. Orme-Johnson and L. C. Davis in "Iron-Sulfur Proteins", Vol. III, W. Lovenberg, Ed., Academic Press, New York, N.Y., 1977, Chapter 2.
- J. Rawlings, V. K. Shah, J. R. Chisnell, W. J. Brill, R. Zimmermann, E. Münck,

- and W. H. Orme-Johnson, *J. Biol. Chem.*, **253**, 1001 (1978).  
 (13) T. D. Tullius, P. Frank, and K. O. Hodgson, *Proc. Natl. Acad. Sci. U.S.A.*, in press.  
 (14) Alfred P. Sloan Foundation Fellow, 1976–1978.

Thomas E. Wolff, J. M. Berg, C. Warrick  
 Keith O. Hodgson,\*<sup>14</sup> R. H. Holm\*

Department of Chemistry, Stanford University  
 Stanford, California 94305

R. B. Frankel

Francis Bitter National Magnet Laboratory  
 Massachusetts Institute of Technology  
 Cambridge, Massachusetts 02139

Received April 13, 1978

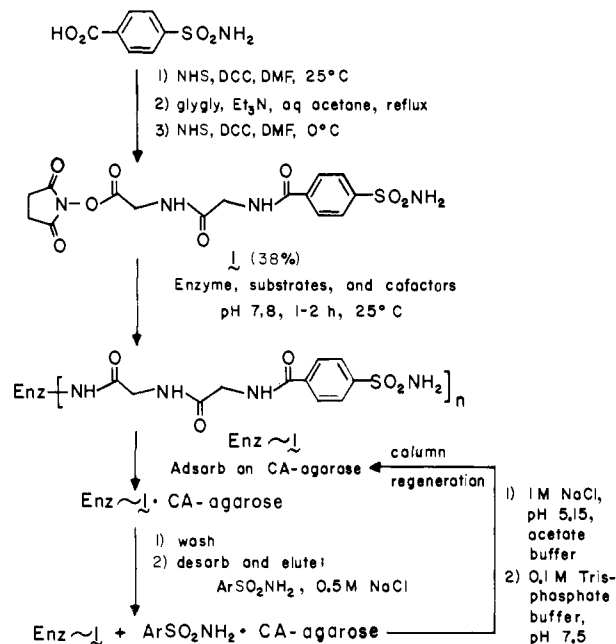
### Generalized Affinity Chromatography: Enzyme-Sulfonamide Conjugates Can Be Isolated by Adsorption on Immobilized Carbonic Anhydrase<sup>1</sup>

Sir:

The practicality of synthetic procedures involving enzymes as catalysts often depends on the ease with which these enzymes can be recovered for reuse.<sup>2</sup> Enzyme recovery is commonly facilitated by immobilization on an insoluble matrix.<sup>3</sup> Immobilization is, however, not always practical, and in several circumstances it may be advantageous to employ a soluble enzyme; when a substrate, product, or cofactor of the enzyme is itself insoluble; when the enzyme is deactivated by immobilization; when association of the enzyme with other macromolecules is required for activity;<sup>4</sup> or when diffusion of substrate through an immobilizing matrix is rate limiting. In principle, recovery of soluble enzymes from synthetic reaction mixtures can be accomplished by a number of conventional techniques for isolating proteins; in practice, each has disadvantages. Ultrafiltration may denature enzymes by shear at, or adsorption on, the filter face; further, it involves apparatus not commonly available in organic laboratories. Gel permeation and ion-exchange chromatographies and protein precipitation techniques are inconvenient when applied to large volumes of solution containing low concentrations of enzyme. Affinity chromatography requires both the development of an appropriate adsorbent for each enzyme,<sup>5</sup> and a preliminary separation of reactants, products, and cofactors which compete with the affinity ligand for the enzyme active site.

To circumvent the limitations of conventional affinity chromatography for enzyme recovery from synthetic reaction mixtures, we have developed a variant on this technique which utilizes a single affinity column to isolate previously modified enzymes from solution. In this procedure, the enzyme of interest is first coupled covalently with an aryl sulfonamide moiety. The enzyme-sulfonamide conjugate may subsequently be isolated easily from reaction mixtures by adsorption on a column of immobilized carbonic anhydrase (CA, from bovine erythrocytes, E.C. 4.2.1.1) and desorption by treatment with solutions of either 0.01 M *p*-toluenesulfonamide or 1.0 M sodium chloride (Scheme I). We have selected carbonic anhydrase as the adsorbing protein for several reasons: it is commercially available and inexpensive; it is easily immobilized in good yield; it does not catalyze reactions likely to destroy probable reactants or products of enzyme-catalyzed synthetic processes; it binds a wide variety of sulfonamide derivatives at its active site with affinities sufficient to make biospecific adsorption easily practical, but not so high as to make desorption difficult or slow ( $K_i \approx 10^{-7}$  M).<sup>6</sup> Since aryl sulfonamides are readily manipulated synthetically, generation of appropriate reagents for the preparation of protein-sulfonamide

**Scheme I.** Preparation and Affinity Adsorption of Enzyme-Sulfonamide Conjugates (Enz-1) (NHS, *N*-hydroxysuccinimide; DCC, dicyclohexylcarbodiimide; DMF, dimethylformamide)



conjugates is straightforward. We have found **17** to give good results (Scheme I).<sup>8</sup>

Compound **1** was coupled with three representative enzymes, glucose 6-phosphate dehydrogenase (G-6-PDH, from *Torula* yeast, E.C. 1.1.1.49), hexokinase (from Baker's yeast, E.C. 2.7.1.1), and lysozyme (from egg white, E.C. 3.2.1.17) (all from Sigma Chemical Co.) to yield enzyme-sulfonamide conjugates according to the following general procedure. A glass vial was charged with 200  $\mu$ L of 2 M HEPES buffer (pH 7.8), 50–100  $\mu$ L of solution containing enzyme (50–100 U of G-6-PDH or hexokinase; 10<sup>5</sup> U of lysozyme), and 40–100  $\mu$ L of solution containing appropriate substrates and cofactors in concentrations well above their Michaelis constants.<sup>9</sup> A 10- $\mu$ L aliquot of a solution of **1** (0.4  $\mu$ mol) in dimethyl sulfoxide was added to the vial, mixed, and allowed to remain at room temperature for 1–2 h. At the end of this coupling period, solutions of G-6-PDH, hexokinase, and lysozyme retained respectively 60, 90, and 90% of their original enzymatic activities.<sup>10</sup> The reaction mixture was loaded onto a column containing CA immobilized on cyanogen bromide activated Sepharose 4B.<sup>11</sup> The column was washed with 50 mL of 0.1 M Tris-phosphate buffer (pH 7.5), to remove unbound enzyme, and then 50 mL of the same buffer containing 0.01 M *p*-toluenesulfonamide ( $K_{i,C_7H_7SO_2NH_2} = 1.0 \times 10^{-7}$  M)<sup>6</sup> and 0.5 M NaCl ( $K_{i,Cl^-} = 0.05$  M)<sup>6</sup> to elute the enzyme-**1** conjugate.<sup>12</sup>

Average yields of activities eluted by the sulfonamide-containing buffer were 50% for G-6-PDH, 80% for hexokinase, and 50% for lysozyme,<sup>14</sup> based on the original activities of the native enzymes prior to the coupling reaction. The proteins eluted with sulfonamide were retained essentially quantitatively on reapplication to the column of immobilized CA, and are assumed to be modified by the covalent attachment of at least one sulfonamide moiety. Figure 1 illustrates representative chromatographic behavior of enzyme-**1** conjugates. These plots indicate that the retention volume of the conjugates is not related to that of the native enzymes and is apparently not influenced by the presence of a large quantity of an unfunctionalized protein (here, horseradish peroxidase) in solution. Moreover, elution of adsorbed enzyme-**1** conjugates from the CA column can be accomplished easily and in high yield.

Since column chromatography may be inconvenient in